

## 7. Laser Ranging Retroreflector

*C. O. Alley, P. L. Bender, R. F. Chang, D. G. Currie, R. H. Dicke, J. E. Faller, W. M. Kaula, G. J. F. MacDonald, J. D. Mulholland, H. H. Plotkin, S. K. Poultney, D. T. Wilkinson, Irvin Winer, Walter Carrion, Tom Johnson, Paul Spadin, Lloyd Robinson, E. Joseph Wampler, Donald Wieber, E. Silverberg, C. Steggerda, J. Mullendore, J. Rayner, W. Williams, Brian Warner, Harvey Richardson, and B. Bopp*

### Concept of the Experiment

The compact array of high-precision optical retroreflectors (cube corners) deployed on the Moon is intended to serve as a reference point in measuring precise ranges between the array and points on the Earth by using the technique of short-pulse laser ranging. The atmospheric fluctuations in the index of refraction prevent a laser beam from being smaller than approximately 1 mile in diameter at the Moon. The curvature of the lunar surface results in one side of the short pulse being reflected before the other side, producing a reflected pulse measured in microseconds, even if the incident pulse is measured in nanoseconds. The retroreflector array eliminates this spreading because of the small size of the array. (The maximum spreading of a pulse because of optical libration tipping of the array will be approximately  $\pm 0.125$  nsec.) In addition, the retroreflective property causes a much larger amount of light to be directed back to the telescope from the array than is reflected from the entire surface area illuminated by the laser beam.

The basic uncertainty in measuring the approximately 2.5-sec round-trip travel time is associated with the performance of photomultipliers at the single photoelectron level. This uncertainty is estimated to be approximately 1 nsec. When the entire system is calibrated and the effects of the atmospheric delay are calculated from local temperature, pressure, and humidity measurements and subtracted from the travel time, where the uncertainty in this correction is estimated to be less than 0.5 nsec, an

overall uncertainty of  $\pm 15$  cm in one-way range seems achievable.

With the  $\pm 15$ -cm uncertainty, monitoring the changes in point-to-point distances from Earth to the lunar reflector (by daily observations for many years) will produce new information on the dynamics of the Earth-Moon system. The present uncertainty of three parts in  $10^7$  in the knowledge of the velocity of light will not affect the scientific aims of the experiment, since it is the practice to measure astronomical distances in light travel time. Primary scientific objectives include the study of gravitation and relativity (secular variation in the gravitational constant), the physics of the Earth (fluctuation in rotation rate, motion of the pole, large-scale crustal motions), and the physics of the Moon (physical librations, center-of-mass motion, size and shape). Some of these objectives are discussed in references 7-1 to 7-4. Estimates made by P. L. Bender of improvements expected in some of these categories are shown in tables 7-I to 7-III.

### Properties of the Laser Ranging Retroreflector

Although the Laser Ranging Retroreflector (LRRR) is simple in concept, the detailed design of a device that would satisfy the stated scientific aims has received much attention. The primary design problem has been to avoid systematic gaps in ranging data expected to result from the extreme variation in thermal conditions on the Moon (from full Sun illumination to lunar night). A preliminary design based on discussions among various members of the investigator group and optical engineers was put

TABLE 7-I. *Lunar orbital data parameters*

Quantity	Present accuracy (approximate)	1.5-m range uncertainty		0.15-m range uncertainty <sup>a</sup>	
		Accuracy	Time, yr	Accuracy	Time, yr
Mean distance	500 m	250 m	1	75 m	0.5
Eccentricity	$1 \times 10^{-7}$	$4 \times 10^{-8}$	1	25 m	1
				$1.5 \times 10^{-8}$	.5
Angular position of Moon with respect to perigee	$2 \times 10^{-6}$	$4 \times 10^{-7}$	1	$4 \times 10^{-9}$	1
Angular position of Moon with respect to Sun	$5 \times 10^{-7}$	$4 \times 10^{-7}$	1	$1.5 \times 10^{-7}$	.5
Time necessary to check predictions of Brans-Dicke scalar-tensor gravitational theory, yr	—	25	25	$1.5 \times 10^{-7}$	.5
				$4 \times 10^{-8}$	1
				8	8

<sup>a</sup>Three observing stations are assumed for periods longer than 0.5 yr.

TABLE 7-II. *Lunar libration and relation of Laser Ranging Retroreflector (LRRR) to center of mass*

Quantity	Present accuracy (approximate)	1.5-m range uncertainty		0.15-m range uncertainty <sup>a</sup>	
		Accuracy	Time, yr	Accuracy	Time, yr
Libration parameters:					
$\beta = (C-A)/B$	$1 \times 10^{-5}$	$3 \times 10^{-7}$	4	$3 \times 10^{-7}$	0.5
$\gamma = (B-A)/C$	$5 \times 10^{-5}$	$2 \times 10^{-6}$	1.5	$3 \times 10^{-8}$	4
Coordinates of LRRR with respect to center of mass:				$1.5 \times 10^{-6}$	.5
$X_1$	500 m	250 m	1	$2 \times 10^{-7}$	1.5
$X_2$	200 m	70 m	1	75 m	.5
				25 m	1
$X_3$	200 m	50 m	3	40 m	.5
				7 m	1
				50 m	.5
				5 m	3

<sup>a</sup>Three observing stations are assumed for periods longer than 0.5 yr.

TABLE 7-III. *Geophysical data determinable from LRRR*

Quantity	Present accuracy (estimated)	1.5-m range uncertainty	0.15-m range uncertainty
Rotation period of Earth, sec	$5 \times 10^{-3}$	$10 \times 10^{-3}$	$1 \times 10^{-3}$
Distance of station from axis of rotation, m	10	3	0.3
Distance of station from equatorial plane, <sup>a</sup> m	20	6 to 20 <sup>b</sup>	0.6 to 2 <sup>b</sup>
Motion of the pole, <sup>a</sup> m	1 to 2	1.5	0.15
East-west continental drift rate observable in 5 yr, <sup>a</sup> cm/yr	30 to 60	30	3
Time for observing predicted 10-cm/yr drift of Hawaii toward Japan, <sup>a</sup> yr	15 to 30	15	1.5

<sup>a</sup> Three or more observing stations are required.

<sup>b</sup> Depending upon the latitude of the station.

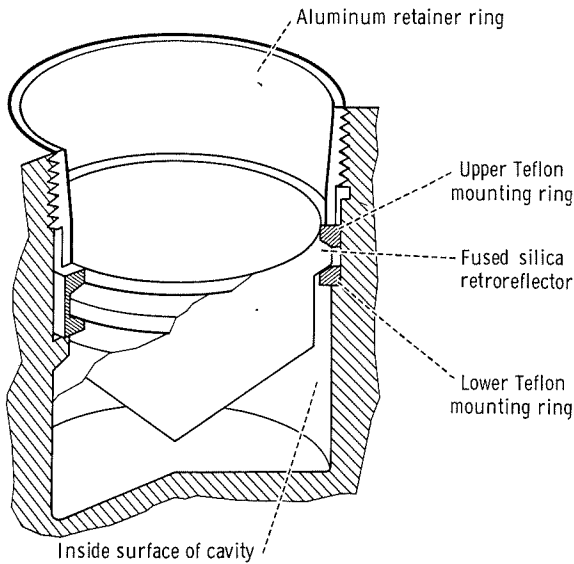
forth by J. E. Faller in a proposal to NASA (ref. 7-5).

The first financial support provided by NASA was used to test the proposed design, which consisted of small solid-corner reflectors made of

homogeneous fused silica. The test and evaluation facilities at the NASA Goddard Space Flight Center were used to simulate the lunar environment. These tests verified that a metal coating could not be used on the reflectors and showed that the

failure of total internal reflection at off-axis angles posed serious problems in mounting the reflectors to maintain small temperature gradients during larger off-axis Sun angles (ref. 7-6).

The tests verified the predicted performance during lunar night and during direct Sun illumination within the total internal reflection region of angles.



The efforts of thermal and mechanical design engineers in close association with members of the investigator group solved the problems and led to the design shown in figure 7-1. The corner reflectors are lightly mounted on tapered tabs between Teflon rings, and are recessed by one-half their diameter into cylindrical cavities in a solid aluminum block. The predicted optical performance, based on thermal analyses under changing lunar conditions, is shown in figure 7-2.

The need for careful pointing of the LRRR toward the center of the Earth libration pattern is shown by figure 7-3, which displays the off-axis response of the recessed corner reflectors. (The curve is the result of averaging over azimuthal orientation and polarization dependence.) The motion of the Earth in the lunar sky because of the optical librations of the Moon is shown in figure 7-4 for the period July to October 1969.

FIGURE 7-1. — Corner reflector mounting.

The alinement in the east-west direction

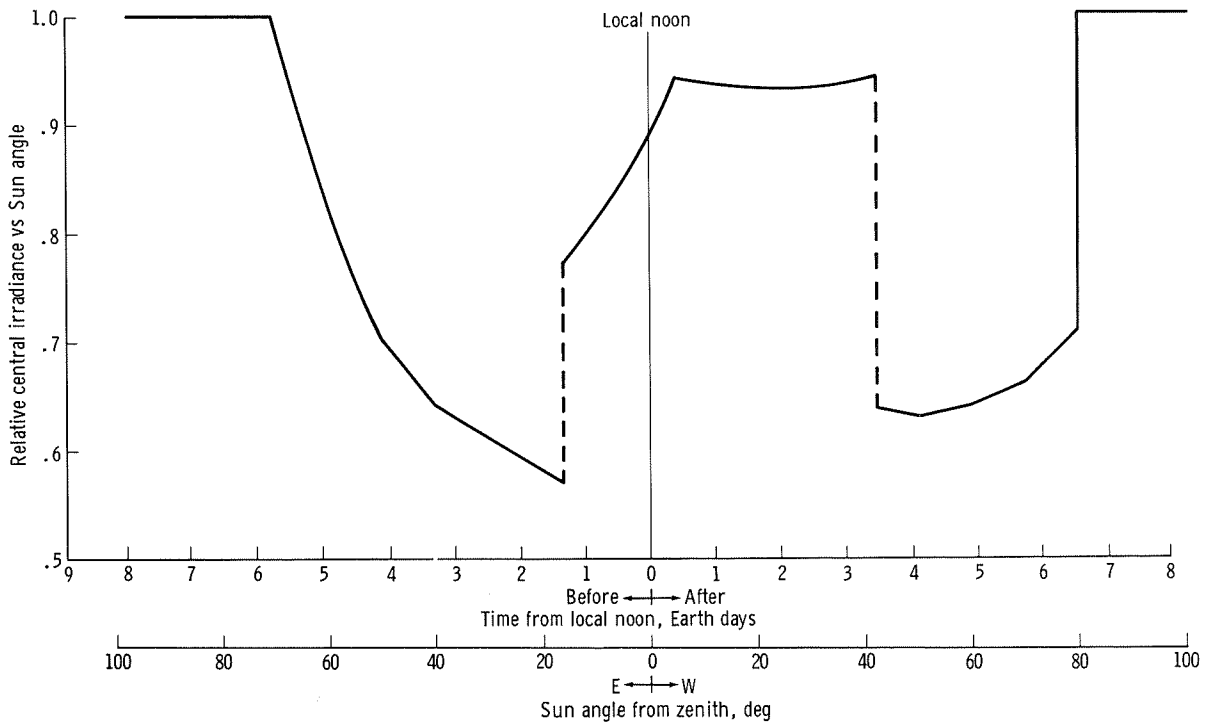


FIGURE 7-2. — Predicted optical performance as a function of Sun angle, from thermal analysis.

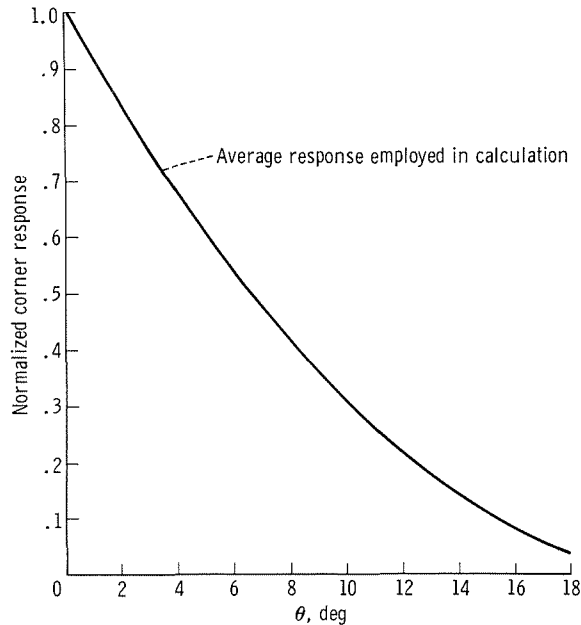


FIGURE 7-3.— Average off-axis performance of recessed circular corner reflectors.

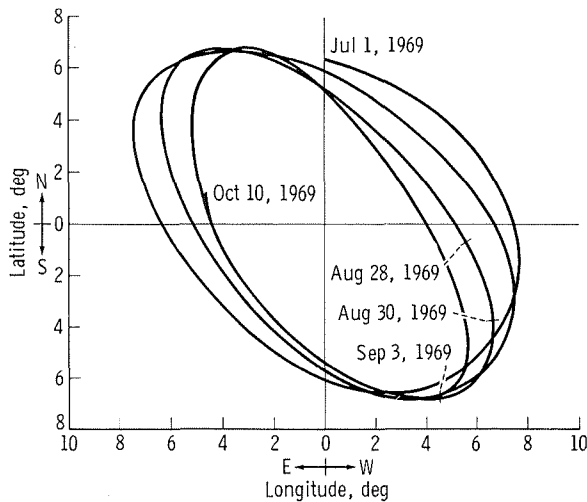


FIGURE 7-4.— Optical librations for the period July to October 1969.

achieved by Astronaut Neil A. Armstrong was within the width of a division on the compass mark. The leveling was within  $0.5^\circ$ , with the bubble oriented toward the southwest. When combined with the worst possible mechanical tolerances of construction, the east-west alinement is  $\pm 0.7^\circ$ , and the overall pointing is within  $1^\circ$  of the center of the libration pattern.

This excellent pointing means that the return will not fall to extremely low values during the extremes of the libration cycle. With the previous information included, the relative expected response from July 20 to September 9, 1969, is shown in figure 7-5. Figure 7-5 is an upper bound for the performance expected.

The flight hardware is shown in figure 7-6. The gnomon, the alinement marks, and the bubble level are clearly shown. In figure 7-7, the LRRR is shown deployed on the Moon.

In tests, each corner reflector which was selected for the flight array exhibited an on-axis diffraction performance greater than 90 percent of that possible for a corner reflector having no geometrical or homogeneity defects. The on-axis, nondistorted performance is conveniently characterized by a differential scattering cross section.

$$\left. \frac{d\sigma}{d\Omega} \right|_{180^\circ} = 5 \times 10^{11} \text{ cm}^2/\text{steradian}$$

which yields the number by which the photon flux density (photons per square centimeter) incident on the reflector array must be multiplied to give the number of photons per steradian intercepted by the telescope receiver. The cross section includes the effect of velocity aberration and is evaluated for a wavelength of 6943 Å.

Observations of returns on August 1 and 3, 1969 (immediately before lunar sunset), and on

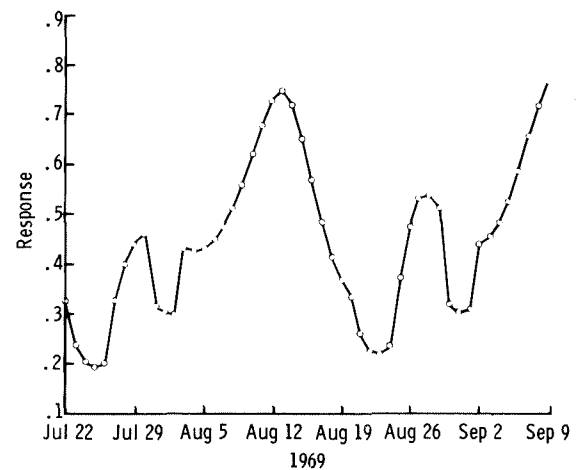


FIGURE 7-5.— Upper bound of LRRR efficiency as a function of time.

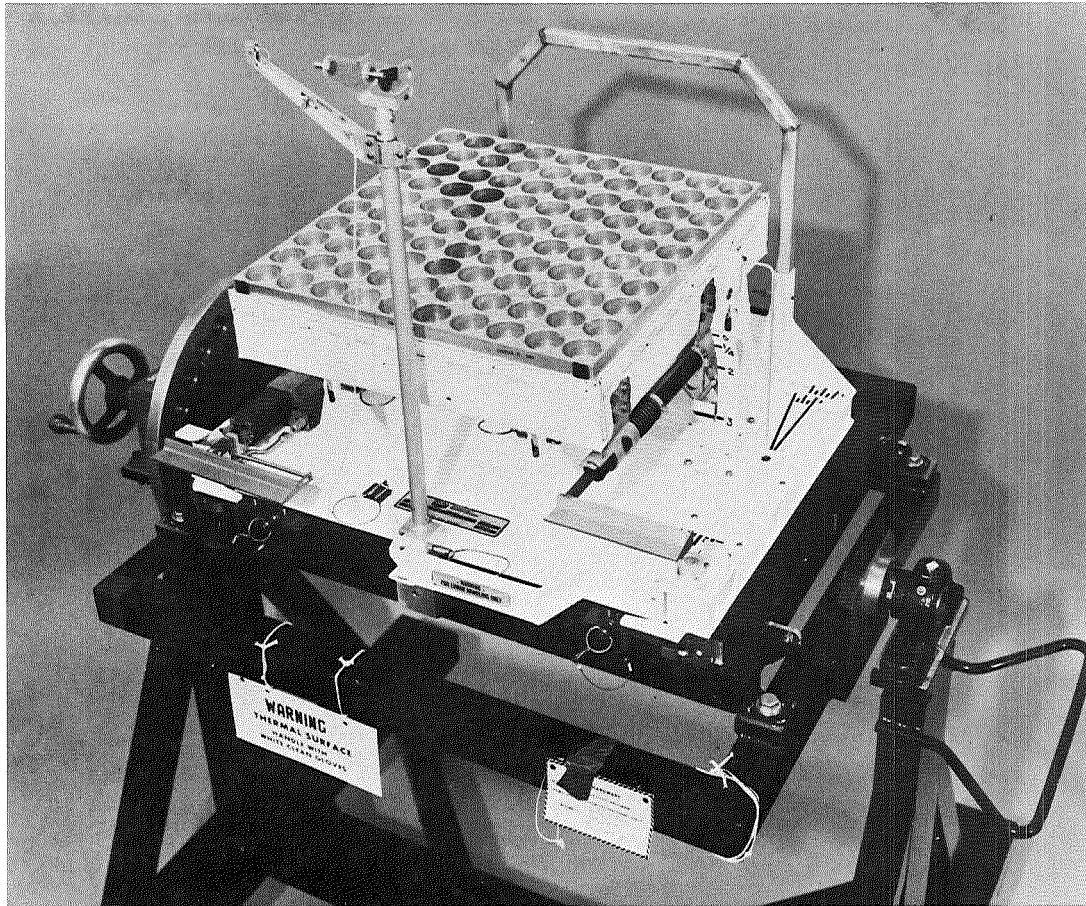


FIGURE 7-6. — The LRRR before stowage in the scientific equipment bay.

August 20, 1969 (immediately after lunar sunrise), show that the mounting (designed to minimize temperature gradients at these large Sun angles) has been successful. Observations of returns on September 3 and 4, 1969 (during lunar night), confirm the expectation that the reflector would perform at very low temperatures and that the differential thermal contractions of the mount and corners do not produce large strains. The survival of the reflectors throughout a lunar night has been demonstrated. Performance degradation, if any, caused by the presence of debris during lunar module (LM) ascent does not appear to be severe.

#### Ground Station Design

A single telescope can be used both as a transmitter and a receiver because the large diffraction pattern resulting from the 3.8-cm-diameter

corner reflectors (the central spot has a diameter on the Earth of approximately 10 miles) allows for a velocity aberration displacement of approximately 1 mile without significant loss of signal. This was one of the major considerations in the design of the LRRR array discussed previously. The 2.5-sec light travel time between transmitting and receiving readily allows the mechanical insertion of a mirror that directs the returning photons collected by the telescope into a photomultiplier detector.

The present beam divergence of short-pulse, high-energy ruby lasers requires the use of a large aperture to recollimate the beam so that the beam is narrowed to match the divergence allowed by the atmospheric fluctuations of the

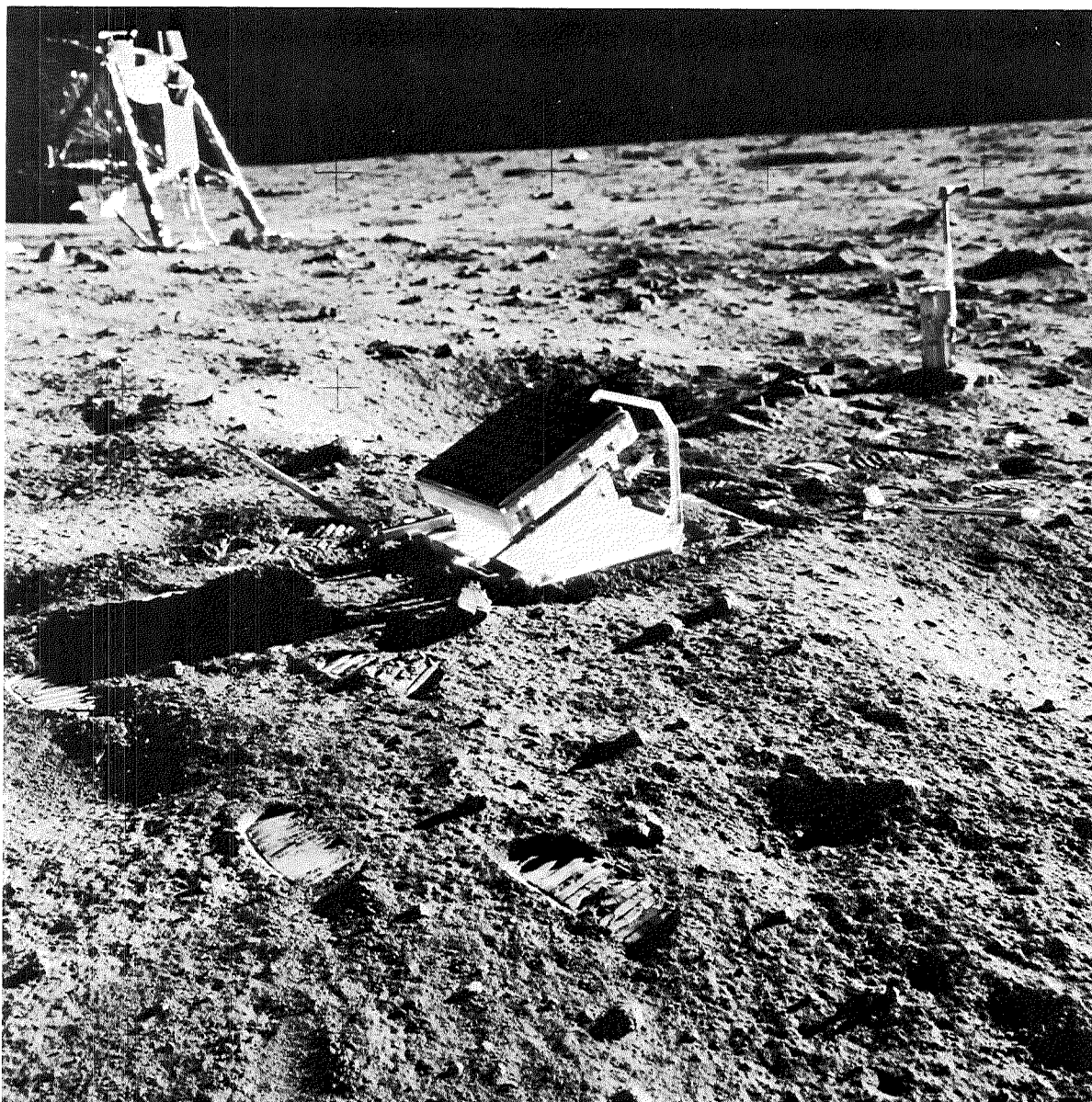


FIGURE 7-7. — The LRRR deployed on the Moon.

index of refraction — typically several seconds of arc. Astronomers refer to this effect as “seeing.” The degree of atmospheric turbulence at an observatory at a given time thus determines the size of the laser beam on the lunar surface, producing a spread of approximately 2 km per sec of arc divergence.

Techniques for pointing such narrow beams to a specific location on the Moon were developed

during the successful Surveyor 7 laser-beam-pointing tests (ref. 7-7). An argon-ion laser beam was brought to a focus in the telescope focal plane at the Moon-image spot that was chosen for illumination. When the laser beam filled the exit pupil of the telescope and matched the  $f$ -number, the collimated beam was projected to the selected location on the Moon and detected by the television camera on the Surveyor

7. For the Apollo laser ranging experiment, the beam is matched into the telescope by using a diverging lens, because it is not possible to focus high-power ruby laser beams in air without causing electrical breakdown. The direction of the projected beam is monitored by intercepting a small portion of the beam with corner reflectors mounted on the secondary mirror-support structure. These reflectors return the intercepted light in such a manner that the light is brought to focus, superimposed on the image of the Moon, at the spot to which the beam is being sent. A beam splitter coated with a highly damage-resistant, multilayer dielectric coating reflects the laser beam into the telescope and transmits the image of the Moon and the laser light intercepted by the telescope corner reflectors into the guiding system (ref. 7-8).

A view of the region of the Moon around Tranquility Base is shown in figure 7-8, which was taken through the guiding eyepiece of the McDonald Observatory 107-in. telescope. The reticle marks used to guide from craters are clearly shown, along with the intercepted laser light. In final alinement, the small circle is made to coincide with both Tranquility Base and the

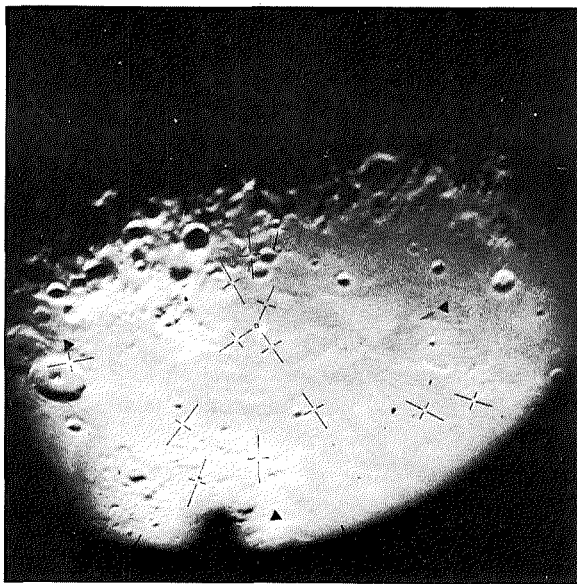


FIGURE 7-8.—View through guiding eyepiece of the McDonald Observatory 107-in. telescope during process of alinement.

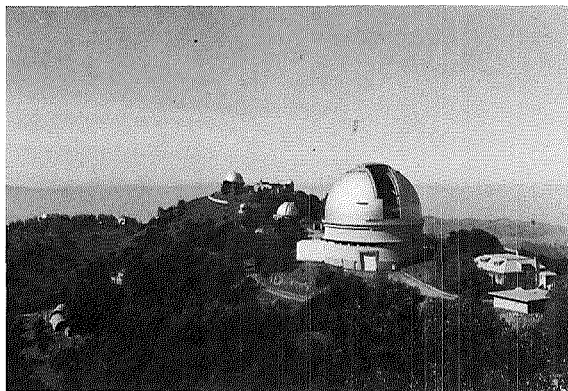


FIGURE 7-9.—Lick Observatory, University of California, at Mount Hamilton, California.

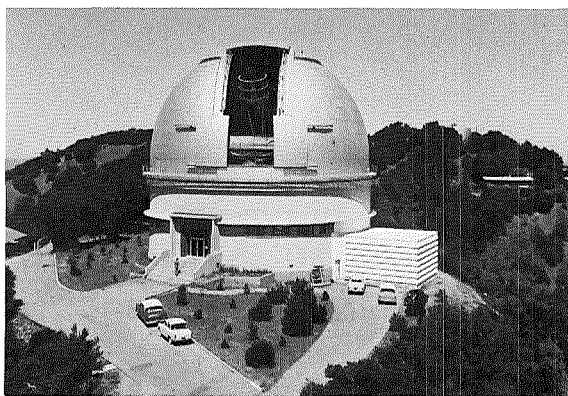


FIGURE 7-10.—Lick Observatory 120-in. telescope dome.

center of the laser spot. The large size of the laser spot is caused by imperfections in the telescope corner reflectors, not by beam divergence. The diameter of the reticle circle is approximately 3.6 seconds of arc. Many craters are not resolved because of poor seeing conditions at the time the photograph was made.

Figures 7-9 to 7-14 are views of the Lick Observatory, University of California, at Mount Hamilton, California; the Lick Observatory 120-in. telescope, the second largest in the world; the McDonald Observatory, University of Texas, at Mount Locke, Tex.; and the McDonald Observatory 107-in. telescope, the third largest in the world. Lasers were mounted in a stationary position at a coudé focus of each instrument.

The Lick Observatory participated in the acquisition phase of the experiment to increase

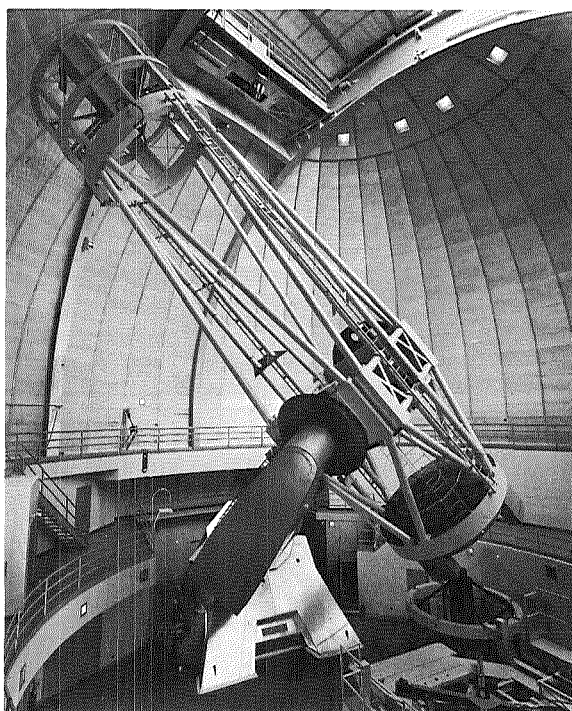


FIGURE 7-11. — Lick Observatory 120-in. telescope.

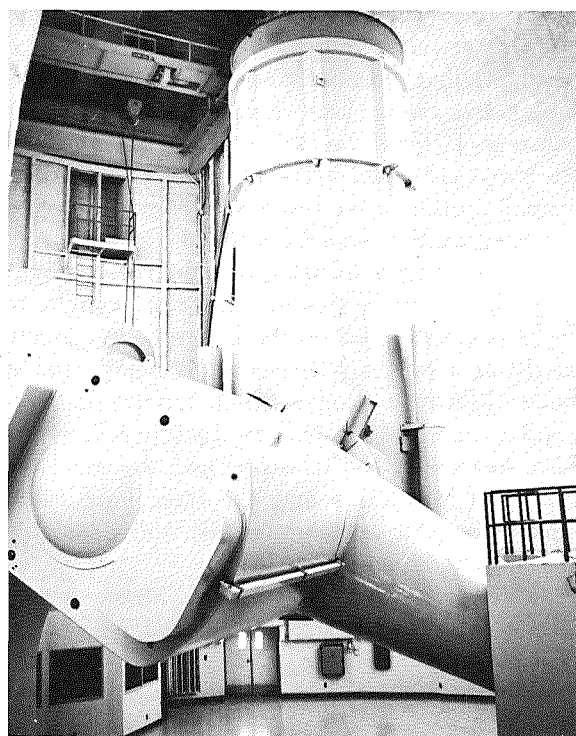


FIGURE 7-13. — McDonald Observatory 107-in. telescope.

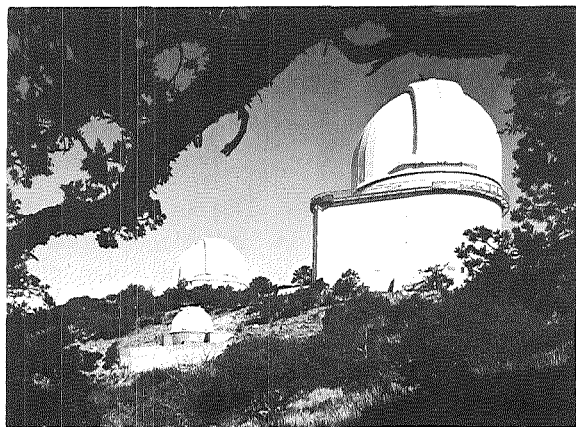


FIGURE 7-12. — McDonald Observatory, University of Texas, at Mount Locke, Tex.

the probability of getting early returns because the weather and seeing there are generally excellent in the summer. Returns at the Lick Observatory, which is no longer in operation, were observed on August 1 and 3, 1969. The McDonald Observatory is equipped to make daily range measurements, weather permitting, for years. Re-

turns were observed on August 20, September 3, September 4, and September 22, 1969, at the McDonald Observatory.

### Observations at the Lick Observatory

#### System A

The ranging system at the Lick Observatory consisted of a giant-pulse, high-powered ruby laser (operated at the coudé focus) which was optically coupled through the 120-in. telescope and could be fired at 30-sec intervals. The angular diameter of the outgoing beam was approximately 2 seconds of arc and made a spot of light on the Moon approximately 2 miles in diameter. The return signal was detected by a photomultiplier that was mounted at the coudé focus behind a 10-second-of-arc field stop and a narrow (0.7 Å) filter, which were used to reduce the background illumination from the sunlit Moon. A time-delay generator (TDG), initiated by the firing of the laser, was used to activate the acquiring electronics approximately 2.5 sec (the Earth-Moon round-trip time for light) later. The



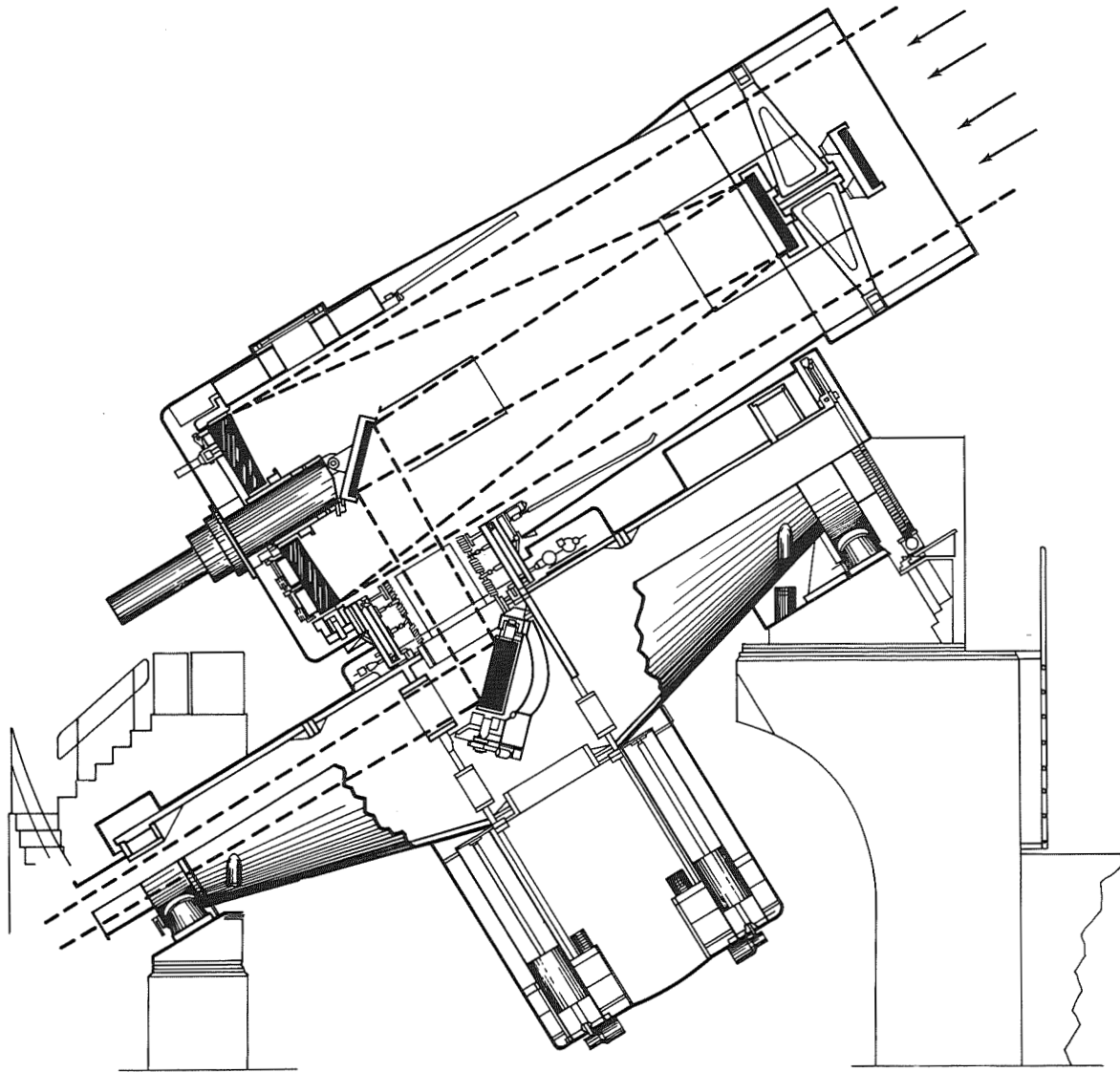


FIGURE 7-14. — Optical path in the McDonald Observatory 107-in. telescope.

delay generator was set for each shot by using the LE 16 ephemeris. (See the section of this report entitled "The Lunar Ephemeris: Predictions and Preliminary Results.")

Following the pulse produced by the TDG, the output pulses from the photomultiplier were channeled sequentially into 12 binary scalers. Each scaler channel had a dwell time that was adjustable from 0.25 to 4  $\mu\text{sec}$  (ref. 7-8). The routing of the pulses to the scalers was such that a pulse arriving within 0.1  $\mu\text{sec}$  of the end of a channel would also add a count to the following

channel. The scalers then contained a quantized summary of the detector output for a short time interval centered on the expected arrival time of the reflected signal. After each scaler cycling following a laser firing, a small online computer read the contents and reset the scalers. The computer stored the accumulated count for each of the scalers and provided a printed output and a cathode-ray-tube display of the data.

Scattered sunlight from the lunar surface produced a random background that slowly filled the 12 time channels. Because the return from

the retroreflector occurred with a predetermined delay, the channel that corresponded in time to the arrival of the signal accumulated data at a faster rate than the other 12 channels. Figure 7-15 illustrates this point by showing the way in which the data actually accumulated during run 18. Following acquisition on the night of August 1, 1969, 169 shots were fired. Range gate errors occurred on 27 shots, and 22 shots were fired with the telescope pointed away from the reflector. For the remaining 120 shots, approximately 100 above-background counts were received. These results represent a return expectation in excess of 80 percent and show that all parts of the experiment operated satisfactorily. Assuming a Poisson distribution of the recorded photoelectrons, the returns correspond to an

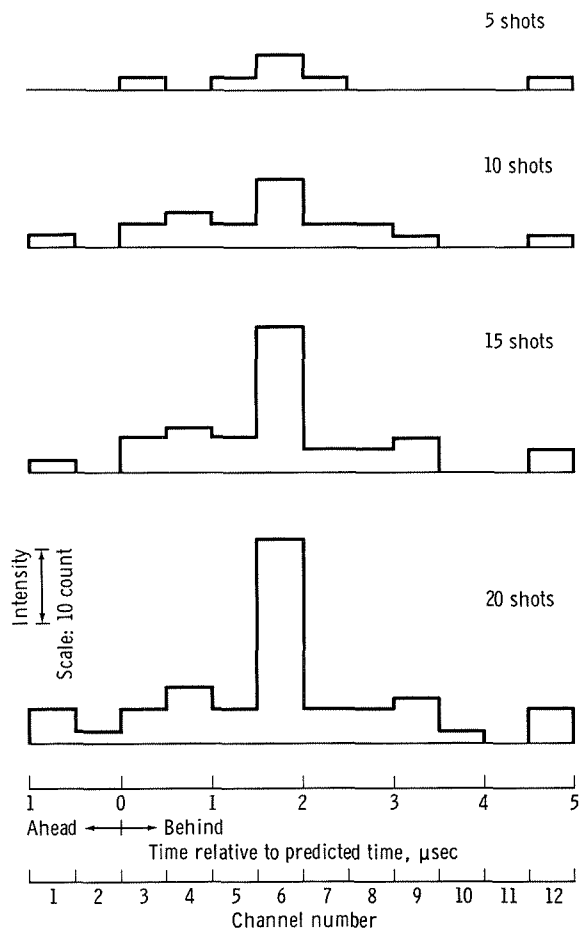


FIGURE 7-15.—Histogram showing the growth of the retroreflected signal in channel 6.

average of 1.6 detectable photoelectrons per shot. This number is a lower limit to the true average because interference effects and guiding errors probably reduced the number of returns that were recorded. The strength of this signal and the lack of “spill” into adjacent channels clearly show that the signal did not come from the “natural” lunar surface, from which the return would be distributed over approximately 8  $\mu$ sec. The timing of the trigger from the TDG relative to Mulholland’s ephemeris was changed three times, and the channel widths were decreased from 2 to 1  $\mu$ sec and then to 0.5  $\mu$ sec. After each change, the signal appeared in the appropriate channel. The data from runs 10 to 21, the interval from the first acquisition to the close of operation, are shown in table 7-IV. Nine runs containing 162 shots were made before acquisition.

Figure 7-16 shows a plot of the data taken from table 7-IV. Runs 12 and 14 have not been plotted in figure 7-16 because errors in setting the TDG invalidated the timing. During run 19, the telescope was not pointed at the reflector, and no returns were seen. Because of a fortuitous splitting of the return between two channels on two runs, an effective timing precision of 0.1  $\mu$ sec was achieved. This precision is equivalent to a range error of approximately 15 m. In figure 7-16 an apparent drift in the time the returns were detected, relative to Mulholland’s predictions, is shown. The drift was caused by the 120-in. telescope being located approximately 524 m east of the locations given for the Lick Observatory in the American Ephemeris and Nautical Almanac. A curve showing this correction to the original ephemeris is given in figure 7-16. Translation of this curve along the ordinate is allowable, and the amount of time gives the difference between the observed range and the predicted range. When the correct coordinates are used, the observations agree with the predicted curve.

#### System B

The primary function of acquisition system B at the Lick Observatory was to locate the deployed LRRR in range and position. System B was not intended to satisfy the long-term objectives of the lunar ranging experiment; however,

TABLE 7-IV. Log of observation data showing acquisition

Run	Total counts												No. of shots	u.t. for middle of run, hr:min	Channel width, $\mu$ sec	Time of first channel <sup>a</sup> $\mu$ sec
	Channel															
	1	2	3	4	5	6	7	8	9	10	11	12				
10	12	8	16	18	12	14	10	17	13	<sup>b</sup> 27	12	12	20	10:21	2.0	-20
11	12	12	12	11	11	6	13	11	14	<sup>b</sup> 26	10	14	14	10:32	2.0	-20
12	(c)	(c)	(c)	(c)	(c)	(c)	(c)	(c)	(c)	(c)	(c)	(c)	16	-	2.0	-10
13	13	8	8	12	7	<sup>b</sup> 18	11	5	6	7	8	12	13	11:04	2.0	-10
14	(c)	(c)	(c)	(c)	(c)	(c)	(c)	(c)	(c)	(c)	(c)	(c)	6	-	1.0	-10
<sup>d</sup> 15	4	3	3	5	4	<sup>b</sup> 17	6	8	10	5	6	8	18	11:23	1.0	-5
16	1	1	2	2	<sup>b</sup> 6	3	3	1	2	1	3	2	10	11:36	.5	-1
17	6	3	4	2	<sup>b</sup> 11	<sup>b</sup> 9	2	7	2	4	2	5	16	11:45	.5	-1
18	3	1	3	5	3	<sup>b</sup> 19	3	3	4	1	0	4	22	12:03	.5	-1
<sup>e</sup> 19	3	3	3	10	4	3	5	2	5	5	8	5	22	12:19	.5	-1
<sup>f</sup> 20	2	1	1	0	3	4	<sup>b</sup> 6	2	4	2	2	4	10	12:23	.5	-1
21	5	2	2	3	2	1	<sup>b</sup> 12	<sup>b</sup> 11	3	4	5	2	22	12:45	.5	-1

<sup>a</sup> With respect to ephemeris predictions.

<sup>b</sup> Channel in which return was expected.

<sup>c</sup> Range-gate errors invalidated data.

<sup>d</sup> Data from three shots with erroneous range gates deleted from tabulation.

<sup>e</sup> Telescope pointed 16 km south of reflector.

<sup>f</sup> Thin clouds noted near Moon.

System B was designed to be a sensitive, moderately precise, semiautomatic, high-repetition rate system using existing off-the-shelf equipment wherever possible.

System B was composed of several essentially independent subsystems. These subsystems were the laser-transmitter/power-supply assembly, the receiver-detector ranging system, the range gate generator and data control and recorder system, and the time standard system.

The laser transmitter uses oscillator and amplifier heads employing a conventional rotating-prism, bleachable-absorber, "Q-switch" mechanism. The oscillator and amplifier heads are identical and use 110-mm-long, 15-mm-diameter Brewster-Brewster rubies. An existing laser system that was modified for this program was capable of operation at 10 J at 3-sec intervals with a pulse width of 60 to 80 nsec.

For operation at the Lick Observatory, modification of the laser system required the incorporation of all normal transmit-receive ranging functions and of a boresight capability onto the laser case. An optical-mechanical assembly (fig. 7-17) was designed to be attached to the laser case. The exiting laser beam passed through a beam splitter, which was oriented at Brewster's angle for minimum reflection of horizontally

polarized light. The small fraction of light scattered or reflected from the beam splitter was detected by an FW 114A biplanar photodiode. The output of the photodiode was used for the range measurement initiation pulse and for monitoring the operation of the laser. The beam splitter was also used to couple a vertically polarized helium-neon laser beam along the same axis as the ruby beam. A helium-neon laser was mounted parallel to the ruby laser, and the resultant beam was expanded by a small autocollimator and then reflected by a mirror mounted parallel to the beam splitter. The reflected beam was then rereflected by the beam splitter along the laser axis. The laser produced an elliptical cross-section beam that was corrected and expanded to 50 mm in diameter by the Brewster entrance prism telescope. The 50-mm exit beam was reflected at right angles onto a 50-mm-aperture F39 lens that was positioned at the appropriate place with respect to the coudé focus of the 120-in. telescope optical system.

The returning energy follows essentially the same path as the transmitted energy. A flip mirror, actuated by a small solenoid, reflects the returning signal after the signal is passed through the correcting telescope to a field-limiting lens and aperture. The aperture in the field-limiting

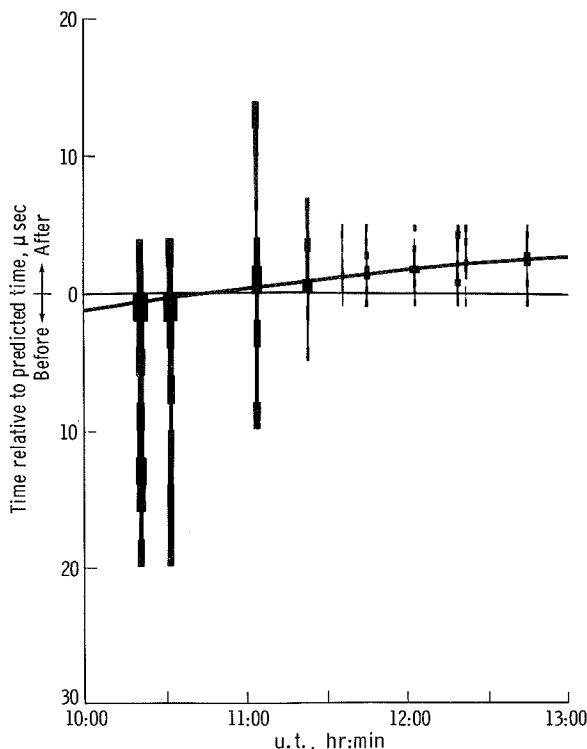


FIGURE 7-16.— Three-dimensional figure showing the time of the run (abscissa), the range window during which the equipment was open for receiving data (ordinate), and the number of counts in each channel (width of the bar). It is clear that in each run in which returns were expected they were seen in the correct channel. During run 19 (third from right-hand end), the telescope was pointed away from the reflector, and no returns were seen.

system is sized for a 10-second-of-arc field of view in space. Light passing through the aperture is collimated and passed through a 2.7-Å bandpass filter. The light is divided into two equal beams by a dividing prism; then, the beams of light enter the enhancement prism on each of the two photomultipliers.

Two detectors (operating in coincidence) and a range gate were used to eliminate as much extraneous background noise as possible. Type 56 TVP photomultipliers used enhancement prisms to allow multiple reflection of the entrance light from the photocathode. The output of each photomultiplier tube was discriminated and shaped with an EGG T105/N dual discriminator. Because theoretical considerations indicate that only a few photoelectrons occur for each

transmitted pulse, the discriminator was used to stretch each detected pulse by the length of the transmitted pulse. A coincidence overlap equal to the transmitted pulse duration was necessary because, lacking discrimination, a photoelectron from each photomultiplier tube could be related to any time within the transmitted pulse duration. The outputs of the discriminators were AND'ed in the EGG C102B/N coincidence module.

The actual range measurement (fig. 7-18) was made with a 1-nsec time-interval counter. The time-interval counter was started by the photodiode output each time the laser transmitter operated. The discriminators and the stop channel of the time-interval unit were disabled by the range gate until the expected time of arrival of the reflected laser pulse. If both photomultiplier tubes detected a photoelectron within the coincidence resolving time of the EGG C102B/N, the output would stop the time-interval unit.

The photodiode signal was used in two other measurements. First, the signal was used to stop a 100- $\mu$ sec-resolution time-interval unit that was started by the "ontime" timing signal from the real-time clock. This measurement determined the time, to the nearest 100  $\mu$ sec, of the range measurement. The pulse was also converted, monitoring the overall performance of the laser during the operation.

System B was controlled and operated by a special digital logic assembly. This device (fig. 7-19) generated laser fire signals and the range gate window, sampled all measurement devices for information, and recorded the information. One of the most important aspects of the operation is the generation of the range gate window, based on knowledge of where the retroreflectors should be. Furthermore, because this information may not be as accurate as required, it is necessary to change the information essentially in real time. The range gate window was generated with an externally, as well as manually, programmed delay pulse generator. The programmed input for the delay pulse generator was obtained from a lunar prediction drive tape containing the expected round-trip time interval to the lunar surface for every 3 sec of time. A digital comparison between the command time on the tape and real time was made to maintain the tape in

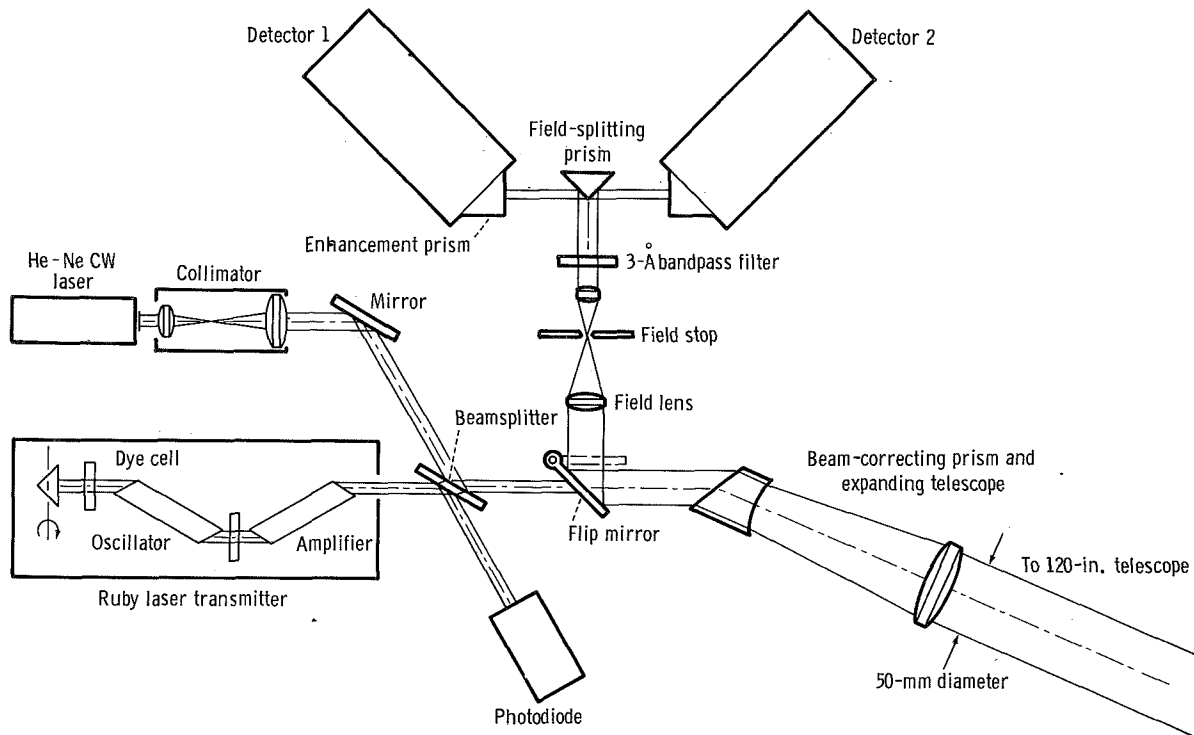


FIGURE 7-17. — Optical schematic of system B at Lick Observatory.

synchronization with real time. The range information on the tape was then stored and transferred to the delay pulse generator prior to each laser firing. The laser firing started the delay pulse generator; and after the predicted delay, a pulse initiated the range-gate-window pulse generator. The range-gate-window length was variable and was used to enable the detector discriminators and the range time-interval unit at the time a return signal was expected.

The measured data were recorded with a multiplexing data gate and standard line printer. The control section generated print commands for each series of measurements at the correct time during the 3-sec cycle period. The control section obtained timing signals from the time standard rack (fig. 7-20). Real time was maintained to an accuracy of  $\pm 10 \mu\text{sec}$  during the operation, by comparing signals from the Loran C chain with the real-time clock using the Loran C synchronization generator.

The system was operated for a period of 1 hr and 45 min on the morning of August 3, 1969, during which the laser was fired 1230 times.

The total number of apparent measured ranges during this period was 98. The low number of returns relative to the number of transmitted pulses is related to a slight (2 sec of arc) misalignment in the detector optical system and to the failure of the delay pulse generator to operate in the externally programmed mode. Furthermore, because returns were not immediately recognized, an angle search was made over a longer time period.

The measured range time could have three possible sources: a return from the retroreflector, a return from the lunar surface, or random noise coincidence from reflected sunlight and background. Statistically, 35 to 50 noise coincidences and approximately 30 lunar surface ranges would be expected in 1200 firings. Because the numbers agree, within acceptable limits, with the total number measured, it is not obvious that returns from the retroreflectors were measured. However, any returns from the retroreflectors should fall within the precision of the system or within 100 nsec with respect to the true range to the package.

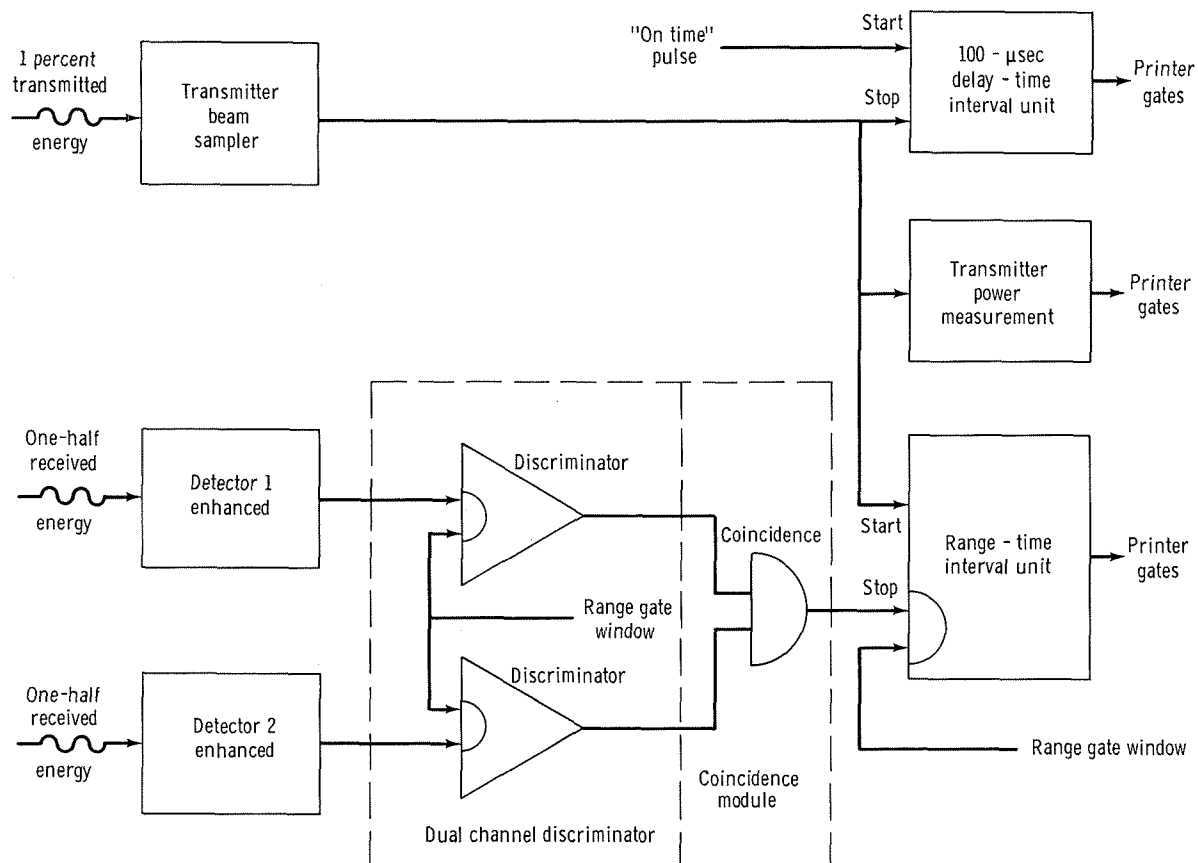


FIGURE 7-18. — Receiver and ranging section.

The observed range time measurements were compared arithmetically with the predicted range time and then linearly corrected because of a known parallax error. The parallax error occurred because a different site was used for the range predictions. The linear correction was performed by taking the initial range residuals and fitting (in a least squares sense) a first-order polynomial to the residuals. Then, only those residuals occurring within a certain range of the polynomial were used to redefine the polynomial. This technique was used successively three times to generate a polynomial about which 11 of the measured ranges had a root mean square of 45 nsec. Furthermore, because of the parallax error, the coefficients of the polynomial agree with the expected deviations from the predicted range.

The range residuals corrected to this linear equation were used to construct a histogram (fig. 7-21) with 100-nsec intervals from  $-5$  to  $+5$

$\mu$ sec. The data lying outside of the  $\pm 5 \mu$ sec were not displayed because no interval contained more than one point and because no significant bunching was observed. The histogram clearly shows a central peak that cannot be supported by any statistical interpretation other than one assuming returns from the retroreflector.

#### Observations at the McDonald Observatory

The laser in use presently is a custom-built two-stage pockels-cell switched ruby system. Typical operating conditions were as follows:

- (1) Energy: 7 J
- (2) Pulse width: 20 nsec
- (3) Beam divergence: 2.4 mrad (measured at full energy points)
- (4) Repetition rate: once every 6 sec
- (5) Wavelength:  $6943.0 \pm 0.2 \text{ \AA}$  at  $70^\circ \text{ F}$
- (6) Amplifier rod diameter: 0.75 in.

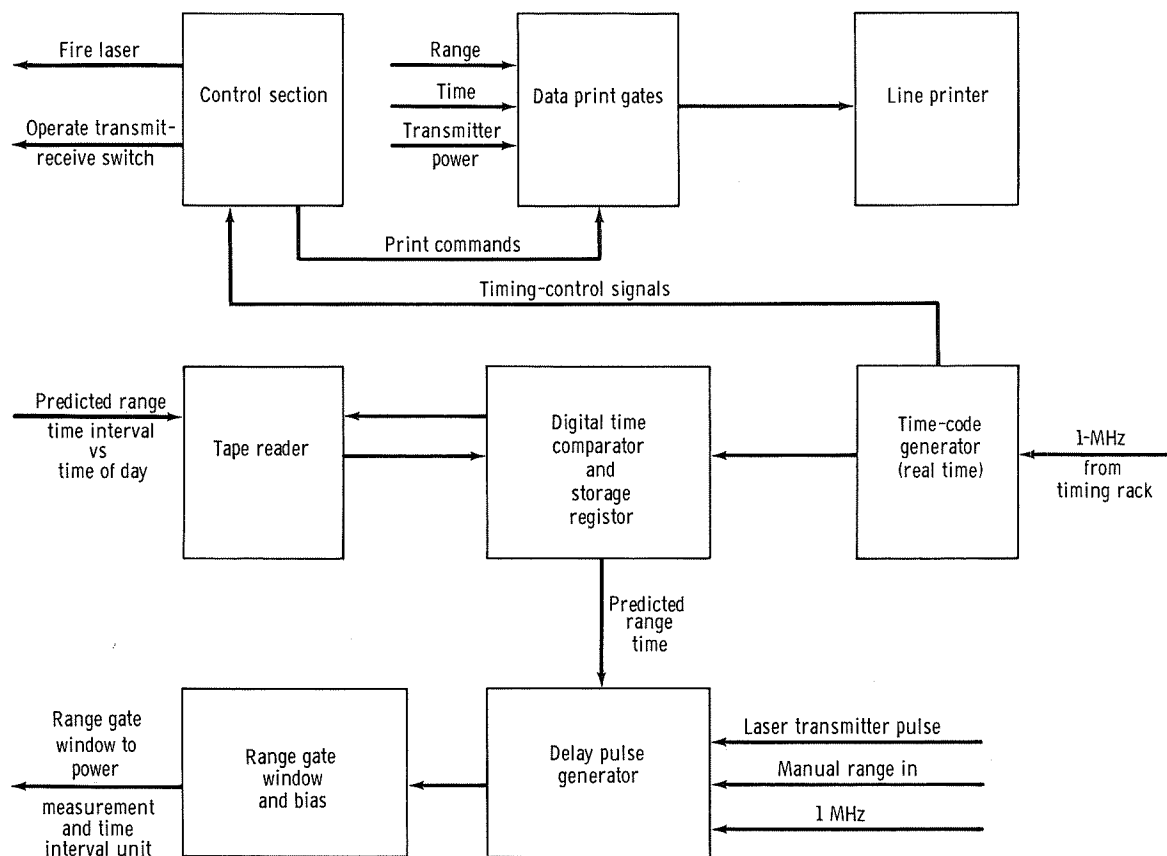


FIGURE 7-19. — Range gate generator and data control.

The detector package contained a photomultiplier that had a measured quantum efficiency of 5 percent at 6943 angstroms and a dark current of 80 000 counts per second. When cooled by dry ice (as during ranging operations), the dark current was 10 000 counts per second. Spectral filters with widths of 3 and 0.7 Å were available. Both filters were temperature controlled. Pinholes restricting the field of view of the telescope to 6" or 9" were commonly used. An air-driven protective shutter was closed during the time of laser firing, opening for approximately 1 sec around the time for receiving returns. The net efficiency of the whole receiver, ratio of photoelectrons produced to photons entering the telescope aperture (with a 3-Å filter), including telescope optics, was measured to be 0.5 percent, using starlight from Vega.

The block diagram of the timing electronics used during the acquisition period is shown in

figure 7-22. The electronics consist of a multistop time-to-pulse-height converter (MSTPHC) for coarse range search covering an interval of 30  $\mu\text{sec}$  with 0.5- $\mu\text{sec}$  bins (ref. 7-8) in addition to the core circuits forming part of the intended subnanosecond timing system. The initial and final vernier circuits of this system were not in use. The range prediction provided by J. D. Mulholland was recorded on magnetic tape at 6-sec intervals. The online computer read the range prediction, set the range gate TDG, and fired the laser within 1  $\mu\text{sec}$  of the integral 6-sec epoch. The TDG activated the MSTPHC, triggered a slow-sweep oscilloscope (the display being recorded on photographic film) and a fast-sweep oscilloscope (recorded on Polaroid), and activated a 10- $\mu\text{sec}$  gate into the time-interval meter (TIM). The computer read the number of counts in the TIM and calculated the difference between this reading and the range prediction, printing out

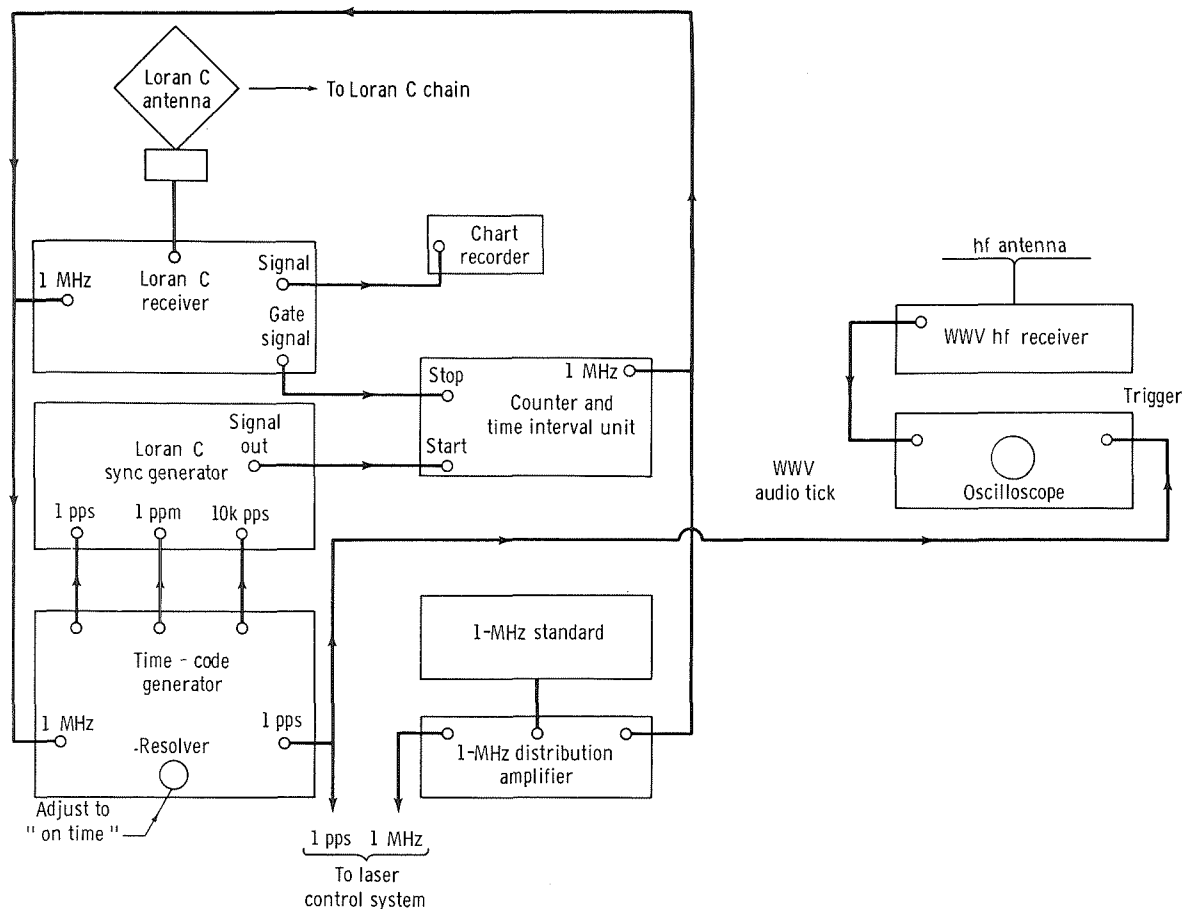


FIGURE 7-20. — Block diagram, time standard system for system B at Lick Observatory.

this difference on the teletypewriter to the nearest nanosecond. The MSTPHC range accuracy depended on the TDG, whereas the TIM range accuracy is entirely independent of the TDG.

The first high-confidence-level return was recorded by the MSTPHC for a 50-shot run at approximately 2:50 Greenwich mean time (G.m.t.) on August 20, 1969 (fig. 7-23). A part of the corresponding TIM printouts is displayed as a histogram in figure 7-24. Here, the origin of the time axis is at the predicted range. The lower histogram shows a portion of the printouts for a 50-shot run taken a few minutes later in which a 5- $\mu$ sec internal delay was introduced. (This delay has been subtracted in the drawing.) Noise scans in which the laser was fired into a calorimeter displayed no buildup. Four other scans recording signals were made in the 50 min before the

Moon sank too low in the sky. Operation earlier in the night had been prevented by cloud cover.

The randomness of the difference between the TIM printout and the ephemeris prediction enabled a statistical reduction of the data even without the vernier circuits designed to interpolate between the 50-nsec digital intervals. The result is a measured round-trip travel time in excess of the Mulholland prediction by  $127 \pm 15$  nsec of time at 3:00 G.m.t., August 20, 1969, from the intersection of the declination and polar axes of the 107-in. telescope. The uncertainty corresponds to  $\pm 2.5$  m in one-way distance.

Return signals were again recorded on September 3 and 4, 1969, with equivalent uncertainty. Round-trip travel times were also shown in excess of the prediction by  $497 \pm 15$  nsec on September 3, 1969, at 11:10 G.m.t. and by



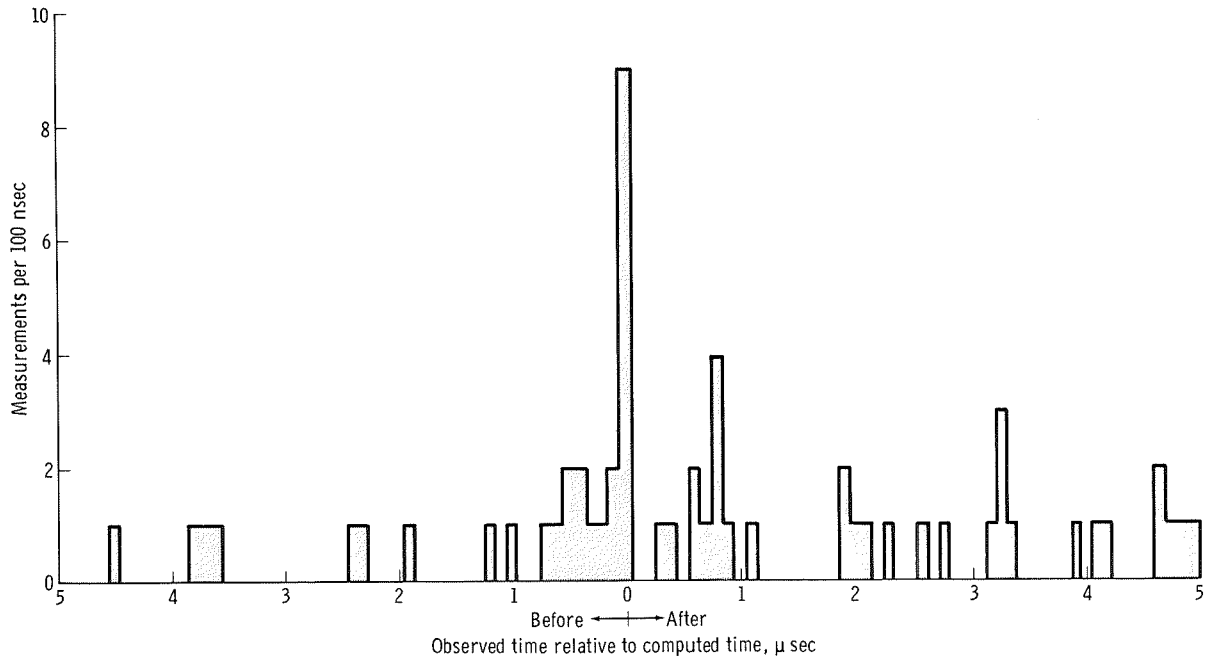


FIGURE 7-21. — Range residuals from system B at Lick Observatory.

$797 \pm 24$  nsec on September 4, 1969, at 10:10 G.m.t. During these observations, Tranquility Base was in darkness, and the computer-controlled drive of the telescope was used successfully to offset from visible craters and track the reflector.

#### The Lunar Ephemeris: Predictions and Preliminary Results

The fundamental input to the calculation of predictions for the LRRR is the lunar ephemeris, which gives the geocentric position and velocity of the lunar center of mass. An ephemeris is being used that was developed at the Jet Propulsion Laboratory (JPL) and is designated LE 16. This ephemeris is believed to be far superior in the range coordinate to any other extant ephemeris. The available observational evidence is meager but supports this belief. The modeling of the topocentric effects relating to the motions of the observatory and the reflector about the centers of mass of the respective bodies is complete and is similar to that used in JPL spacecraft tracking programs. Universal time (u.t.) 1 is modeled and extrapolated by polynomials fit to the instantaneous determinations

by the U.S. Naval Observatory Time Service. The Koziel-Mitielski model is currently being used for the lunar librations.

Coordinates of the telescope and the reflector package are input variables to the prediction program. Reflector coordinates presently used are those derived at the NASA Manned Spacecraft Center from spacecraft tracking of the lunar module, since this dynamic determination is essentially the inverse of the predictive problem and is, thus, more compatible than the selenographic determinations.

It was anticipated that the topographic modeling would be the primary error source in the earliest phase of ranging operations. This belief was based upon the indications from command and service module (CSM) tracking of Apollo 8 and Apollo 10, both of which indicated LE 16 ephemeris errors of 40 to 50 m ( $0.3 \mu$ sec), and is based on the knowledge that various estimates of the selenocentric distances of surface locations disagreed by perhaps 2 km for a specific region. The decision to use the dynamic determinations of the location simplified the real-time processes but did not relieve the radial distance uncertainty until laser acquisition was an accom-

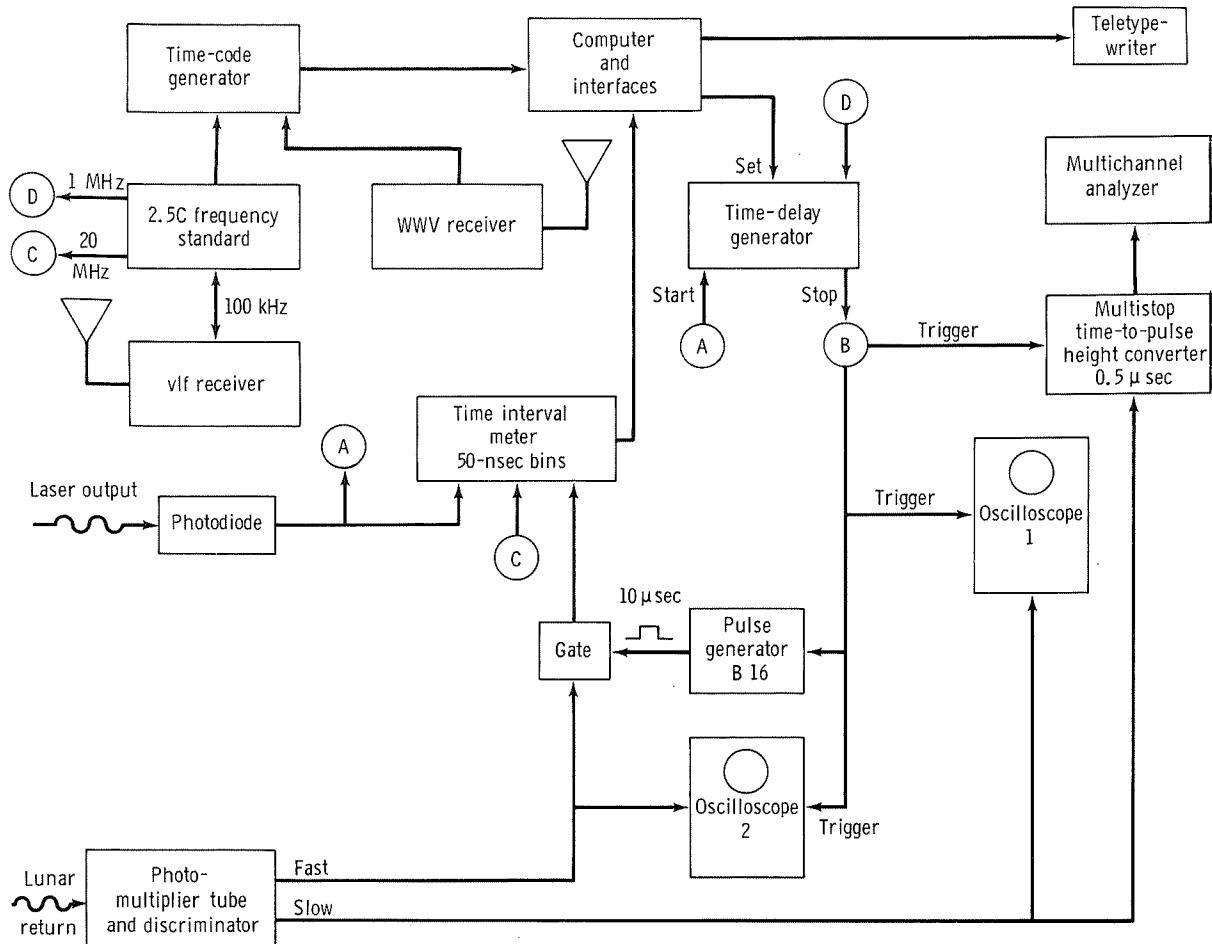


FIGURE 7-22. — Block diagram of McDonald Observatory acquisition and early measurement phase electronics.

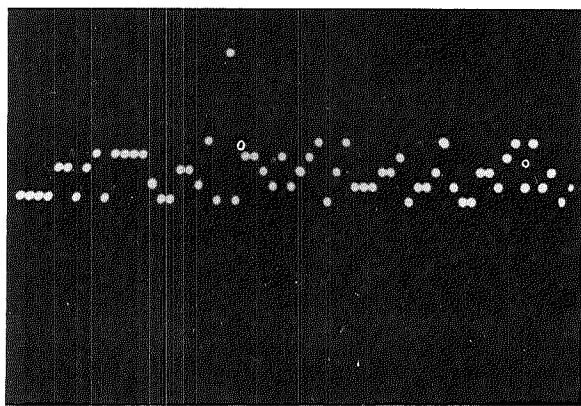


FIGURE 7-23. — MSTPHC display of McDonald Observatory acquisition.

plished fact. As the current "best estimate" of the landing site shifted, predicted ranges were affected by approximately 4 km ( $28 \mu\text{sec}$ ). Site coordinates for Tranquility Base provided by the NASA Manned Spacecraft Center on July 22, 1969, are currently being used.

Tracking information is available on both the CSM and the lunar module during lunar surface operations. The CSM data indicate an ephemeris error not greater than 50 m. Computations of predictions for comparison with the LM ranging data, using the coordinates mentioned previously, show residuals of approximately 2 km, with a drift of 0.3 km in 15 min. The explanation of this anomaly is not yet known, but it seems to be associated with the tracking station location.

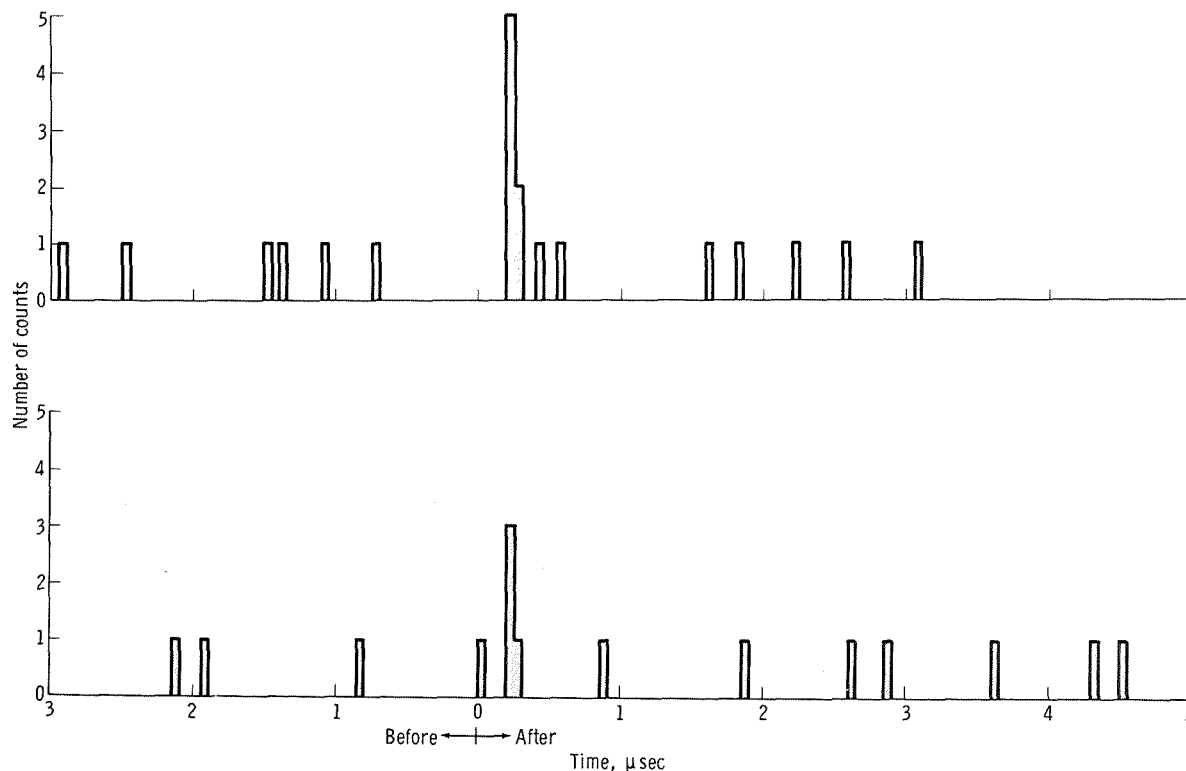


FIGURE 7-24. — Histogram of single-stop TIM readings on two successive 50-shot runs on August 20, 1969, at the McDonald Observatory.

Initial acquisition of the LRRR was accomplished with predictions based on the coordinates of the Lick Observatory, as published in the American Ephemeris and Nautical Almanac. The Lick Observatory 120-in. telescope used in the experiment is actually a distance of approximately 1800 ft from that location, causing drift in the observation residuals. The result of introducing the proper telescope coordinates into the computations is shown in figure 7-25. The residuals relative to the new telescope coordinates appear to be given within  $1 \mu\text{sec}$ . Figure 7-25 is provisional and subject to later refinement. Within the limitations of figure 7-25, these data are consistent with the subsequent observations at McDonald Observatory.

Although it is premature to discuss the data from the standpoint of any meaningful application, one aspect invites speculation and preliminary inference. The three indirect pseudo-observations (range biases on CSM tracking data)

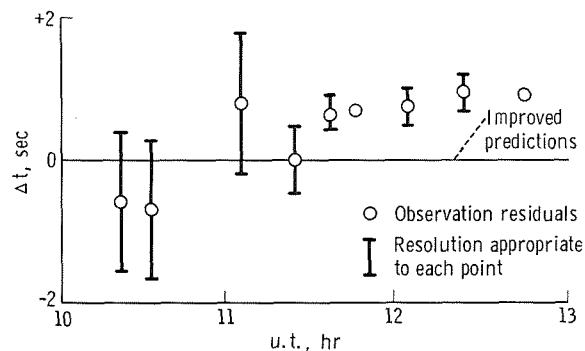


FIGURE 7-25. — Result of using adjusted telescope coordinates for the Lick Observatory. The data are shown for August 1, 1969.

and the first few laser acquisitions yield positive observation residuals. If no observation selection effect is involved, this may be an indication that the ephemeris scaling factor and hence the lunar mean distance requires an adjustment in the seventh place. Such a result would not be

surprising because the uncertainty in the scaling factor is five parts in  $10^7$  (ref. 7-10), based on the results of Mariner spacecraft tracking.

### References

- 7-1. ALLEY, C. O.; BENDER, P. L.; DICKE, R. H.; FALLER, J. E.; FRANKEN, P. H.; PLOTKIN, H. H.; and WILKINSON, D. T.: Optical Radar Using a Corner Reflector on the Moon. *J. Geophys. Res.*, vol. 70, May 1965, p. 2267.
- 7-2. ALLEY, C. O.; and BENDER, P. L.: Information Obtainable from Laser Range Measurements to a Lunar Corner Reflector. Symposium No. 32 of the International Astronomical Union on Continental Drift, Secular Motion of the Pole, and Rotation of the Earth, W. Markowitz and B. Guinot, eds., D. Reidel Publishing Co. (Dordrecht, Holland), 1968.
- 7-3. ALLEY, C. O.; BENDER, P. L.; CURRIE, D. G.; DICKE, R. H.; and FALLER, J. E.: Some Implications for Physics and Geophysics of Laser Range Measurements from Earth to a Lunar Retro-Reflector. Proceedings of NATO Advanced Study Institute on the Application of Modern Physics to the Earth and Planetary Interiors, S. K. Runcorn, ed., John Wiley & Sons (London), 1969.
- 7-4. MACDONALD, G. J. F.: Implications for Geophysics of the Precise Measurement of the Earth's Rotation. *Science*, 1967, pp. 157 and 204-205.
- 7-5. ALLEY, C. O.; ET AL.: Laser Ranging to Optical Retro-Reflectors on the Moon. Univ. of Maryland proposal to NASA, Dec. 13, 1965 (Rev. Feb. 11, 1966); Appendix VII - Design and Testing of Lunar Retro-Reflecting Systems by J. E. Faller.
- 7-6. ALLEY, C. O.; CHANG, R. F.; CURRIE, D. G.; FALLER, J. E.; ET AL.: Confirmation of Predicted Performance of Solid Fused Silica Optical Corner Reflectors in Simulated Lunar Environment. Univ. of Maryland Progress Report to NASA, Oct. 10, 1966.
- 7-7. ALLEY, C. O.; and CURRIE, D. G.: Laser Beam Pointing Tests. Surveyor Project Final Report, Part 2, Science Results. Jet Propulsion Laboratory NASA Tech. Rept. 32-1265, June 15, 1968.
- 7-8. SILVERBERG, E. C.: An Inexpensive Multichannel Scaler With Channel Widths of Less than One Microsecond. *Rev. of Sci. Inst.*, Oct. 1969.
- 7-9. CURRIE, D. G.: Some Comments on Laser Ranging Retro-Reflector Ground Stations. Univ. of Maryland Tech. Rept. 956, Sept. 4, 1968.
- 7-10. MELBOURNE, W. G.; MULHOLLAND, J. D.; ET AL.: Constants and Related Information for Astrodynamical Calculations, 1968. Jet Propulsion Laboratory Tech. Rept. 32-1306, July 15, 1968.

### ACKNOWLEDGMENTS

Responsibility for the design and conduct of the experiment has rested with the following groups: Principal Investigator, C. O. Alley (University of Maryland); Co-Investigators, P. L. Bender (National Bureau of Standards), R. H. Dicke (Princeton University), J. E. Faller (Wesleyan University), W. M. Kaula (University of California at Los Angeles), G. J. F. MacDonald (University of California at Santa Barbara), J. D. Mulholland (JPL), H. H. Plotkin (NASA Goddard Space Flight Center), and D. T. Wilkinson (Princeton University); Participating Scientists, W. Carrion (NASA Goddard Space Flight Center), R. F. Chang (University of Maryland), D. G. Currie (University of Maryland), and S. K. Poultney (University of Maryland).

The following people are responsible for the section of this report entitled "Observations at the Lick Observatory": James Faller and Irwin Winer (Wesleyan University); Walter Carrion, Tom Johnson, and Paul Spadin (NASA Goddard Space Flight Center); and Lloyd Robinson, E. Joseph Wampler, and Donald Wieber (Lick Observatory, University of California). These authors of the "Observations at the Lick Observatory" section wish to acknowledge the efforts of Norman Anderson (Berkeley Space Science Laboratory); Harold Adams, Raymond Greeby, Neal Jern, Terrance Ricketts, and William Stine (Lick Observatory); Barry Turnrose, Steve Moody, Tom Giuffrida, Dick Plumb, and Tuck Stebbins (Wesleyan University); and James MacFarlane, Bill Schaefer, Richard Chabot, James Hitt, and Robert Anderson (NASA Goddard Space Flight Center). Support from funds to the Lick Observatory by NASA grant NAS5-10752 and National Science Foundation grant GP 6310, from funds to Wesleyan by NASA Headquarters grant NGR-07-006-005, and from in-house funds used by Goddard personnel is acknowledged.

The people who are responsible for the section of this report entitled "Observations at the McDonald Observatory" include D. G. Currie, S. K. Poultney, C. O. Alley, E. Silverberg, C. Steggerda, J. Mullendore, and J. Rayner (University of Maryland); H. H. Plotkin and W. Williams (NASA Goddard Space Flight Center); and Brian Warner, Harvey Richardson, and B. Bopp (McDonald Observatory). The authors of this section wish to acknowledge the efforts of Harlan Smith, Charles Jenkins, Johnny Floyd, Dave Dittmar, Mike McCants, and Don Wells (McDonald Observatory); Faust Meraldi, Norris Baldwin, Charles Whitted, and Harry Kriemelmeyer (University of Maryland); and Jim Poland, Peter Minott, Cal Rossey, Jim Fitzgerald, Walter Carrion, Mike Fitzmaurice, and Herb Richard (NASA Goddard Space Flight Center).

Support for the activities at the McDonald Observatory from NASA Grant NGR 21-002-109 to the University of Maryland and from in-house funds at the Goddard Space Flight Center is acknowledged.

J. D. Mulholland (JPL) is responsible for the section entitled "The Lunar Ephemeris."